

**AE 461 Laboratory Note for Experiment # 2**  
**Measurement of Stress using Photoelasticity**

by

**Felix Marrar, Quang Do, Jason Chen, Shanit Dev, Michael Biela, and Jamal Zain**

**TA: Franco Cubas**

**Section AB8, Group G, Tuesday, 5:30 – 7:30 pm**

**March 1st, 2022**

## 1. INTRODUCTION

First discovered by British scientists around the beginning of the 20th century [1], photoelasticity has been used by scientists to determine the stress state of samples. Although photoelasticity analysis can only be applied to birefringent material, it is still useful to understand the possible stress distribution or concentration pattern for certain shapes and holes that otherwise have no analytical solution.

To conduct photoelasticity analysis, a light field or a dark field must be established at the observation location, which serves as the basis of analysis. This step can be easily done with two polarizing lenses. By placing one polarizing lens before the birefringent sample (the polarizer) and one polarizing lens after the sample (the analyzer). If the plane of vibration for the two lenses are crossed, a dark field will be established at the observation end, since the two crossing polarizers will filter all of the light that does not pass the birefringent sample. A light field can be created following the same principle. To further increase the accuracy of observations, it is also suggested to remove isochromatics from the final image, which can be done with two quarter wave plates [2].

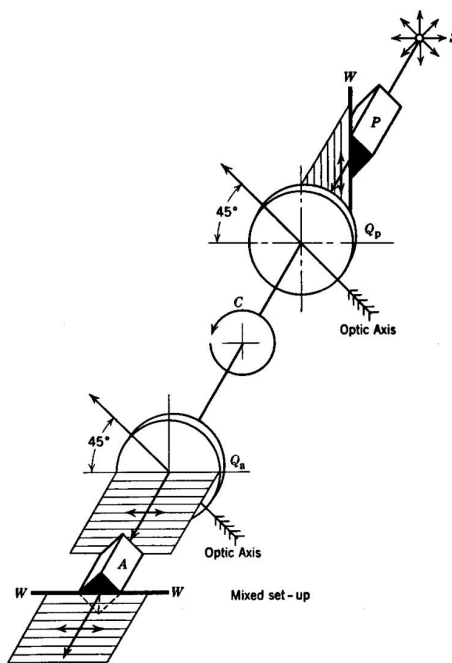


**Figure 1: Light field setup after adding two quarter wave plates and two polarizer**

Once the preliminary preparation is finished, a camera at the end of the light path is used to capture and feed monochromatic video to the computer analysis software for measurements. For this experiment, three beam samples were tested – an unnotched beam, a beam with a circular notch (U-notched), and a beam with a slotted notch (V-notched). Each sample was tested by placing them into the loading apparatus and applying different forces to them, recording the pattern and distance of the fringe from the top of the sample at different force increments. These measurements will allow for calculation of stress levels at and outside the fringe locations using the following equation:

$$\sigma_1 - \sigma_2 = \frac{\delta}{2\pi} \frac{f_\sigma}{t}$$

where

$\sigma_i$  = Principal stress

$\frac{\delta}{2\pi}$  = Retardation of the light

$f_\sigma$  = Material fringe constant

$t$  = Thickness of the material

The retardation of the light caused by the birefringent material in light field follows this mathematical relationship:

$$\frac{\delta}{2} = \frac{\pi}{2}(1 + 2m)$$

where  $m$  is the number of fringes.

With the two equations above, the stress level at each fringe can be easily calculated from its fringe number (counted from the zero fringe), as long as the material fringe constant is known. Besides the fringe pattern and stress level, the magnitude of the force and the dimensions of the mount are also measured to calculate the shear force and moment exerted on the sample. The force and moment on the sample are illustrated by a free body diagram, discussed in more detail in Section 3.

The same procedure was repeated for the round and slotted notch beams, but the dimensions of the notch for the two samples were measured using the Rincon HD software. For the round notch

sample, the diameter of the notch is the key dimension that needs to be measured, while for the slotted notch sample, the angle of the V shape and the length of the slot before the V shape needs to be measured. The dimensional data of the two notches is critical to obtain the analytical solution of stress near these notches. The analytical solution will then be compared to the extrapolated solution (based on distance of the fringe from the top and the stress level at that fringe) in Section 3.

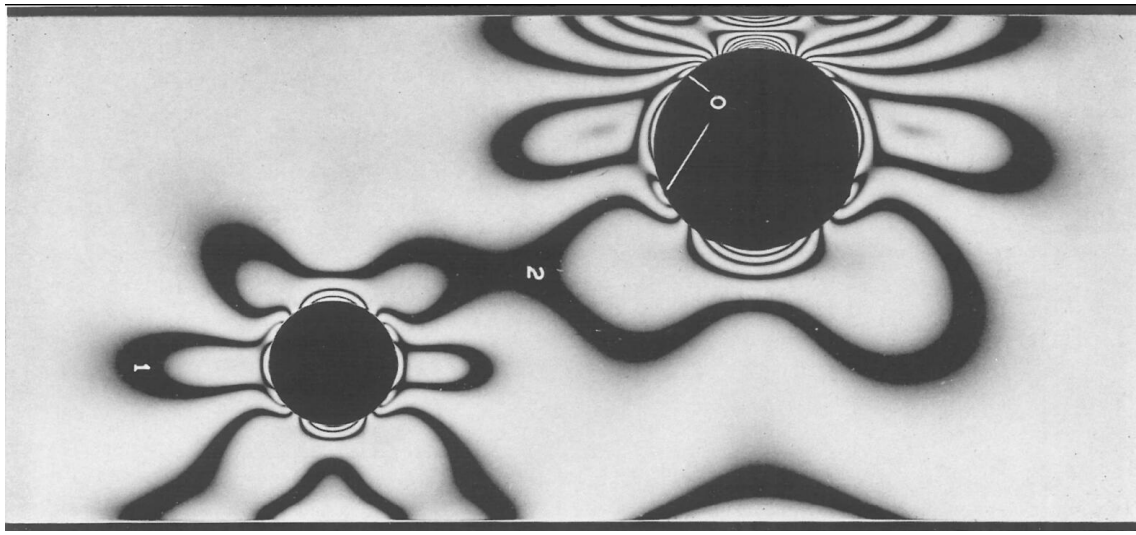


**Figure 2: an example of photoelasticity with complex stress concentration**

## 2. APPARATUS

The apparatus of the experiment contains polarizer, quarter wave plates, light source, sample mount, force sensor, stress applier, computer analysis system, and observation camera. Here is a general schematics of the system:

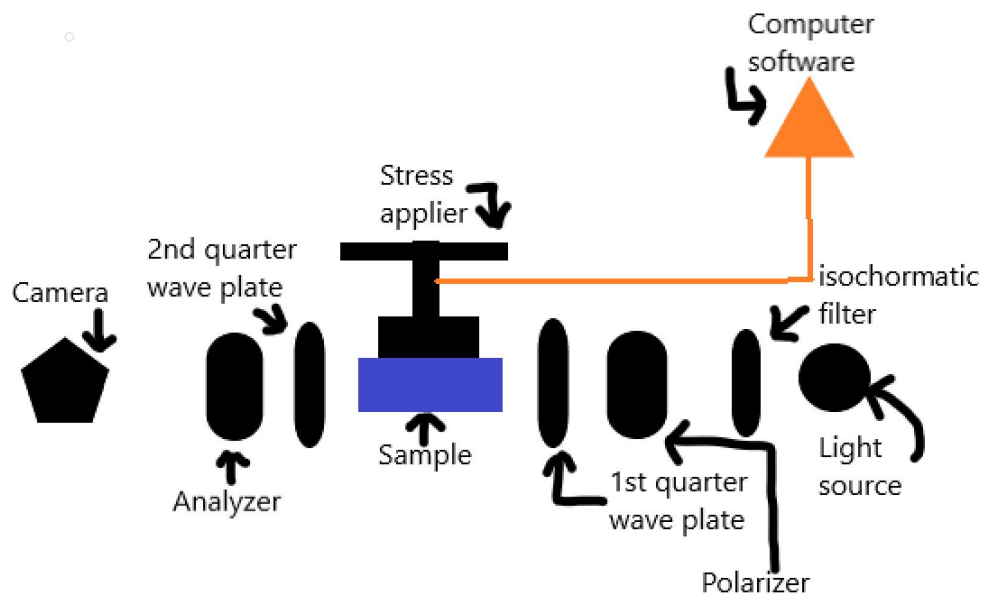


**Figure 3: Schematics of the general experiment setup**

And here are the corresponding elements in real life set up:

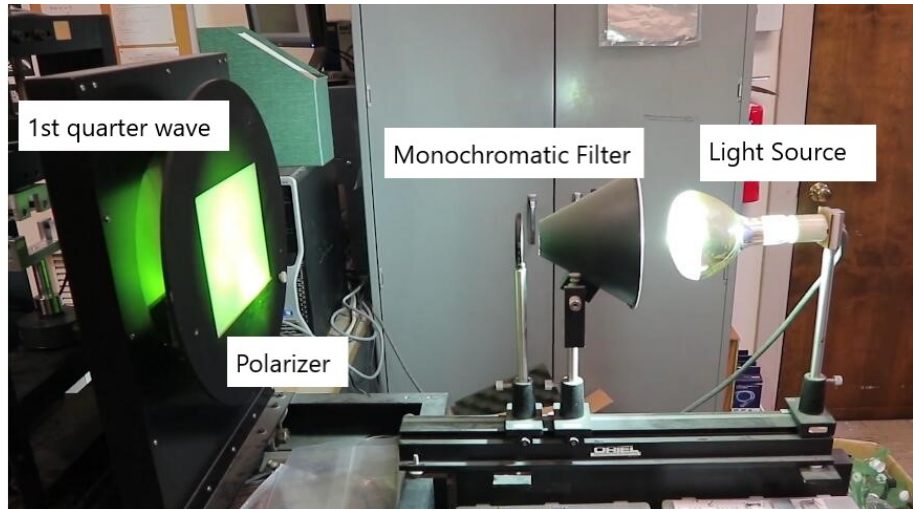


**Figure 4: First part of annotated real experiment set up**

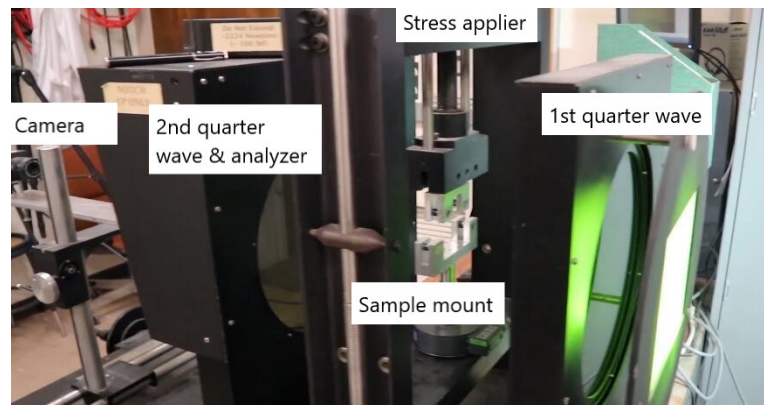


**Figure 5: Second part of annotated real experiment set up**

Below are the samples that will be tested on the mount:

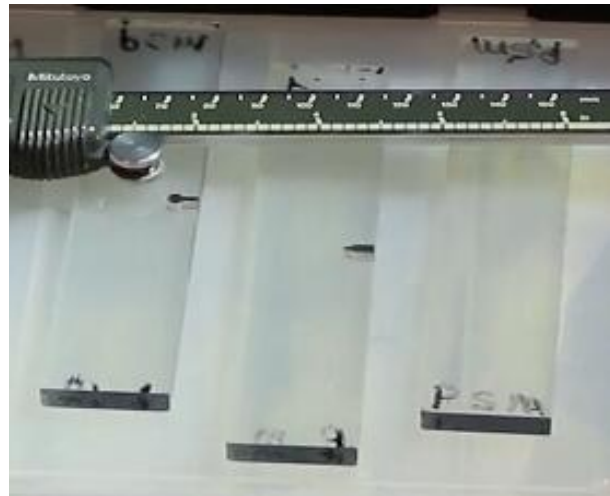


**Figure 6: Image of the testing samples**

**Table 1: Equipment and Sample[3]**

No.	Item	Size/Range/Capacity	Accuracy	Use in Experiment
1	Light source	length 6", width 3", height 3"	-	Provide light source for imaging
2	Monochromatic filter	radius 2"	-	Only green light will pass through the filter for monochromatic image
3	Polarizer and Analyzer lens	length 8", width 8", thickness 0.1"	-	To create light/dark field
4	Quarter wave plate	radius 5"	-	Eliminate isochromatics for better imaging
5	Sample mount	length 6", width 3", height 3"	-	Provide stable platform for the experiment
6	Stress applier	-	-	Apply stress to the samples on the sample mount
7	Force sensor	-	$\pm 1\text{N}$	Measures the applied force to the sample
8	Camera system	length 5.5", width 3", height 3"	HD resolution, 8 bit color depth	Record the final fringe image out of the analyzer
9	Rincon HD software	-	Unspecified accuracy for measuring	Measures the number and distance of fringes from the top of the sample
10	Birefringent samples	3x samples: unblemished, round notch, slotted notch	-	Will be placed on sample mount and be applied stress for photoelasticity analysis

### 3. RESULTS AND DISCUSSION

#### 3.1 Shear and Bending Moment Diagrams

A free body diagram for the unnotched beam was created based on the dimensions of the loading apparatus recorded during the lab, and is shown in Figure 7.

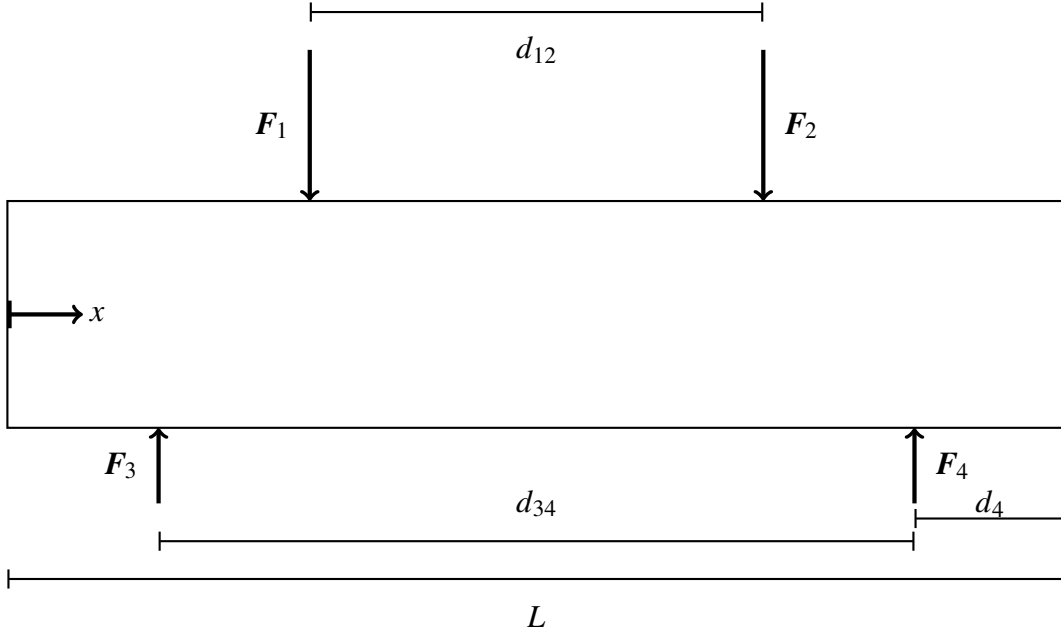


**Figure 7: Free-Body Diagram for Unnotched Beam**

The method of cuts was used to solve for the shear force and bending moment as a function of distance along the length of the beam. The free body diagram for the beam satisfies the following conditions:

$$\sum F_z = 0 \quad \sum M_y = 0 \quad (1)$$

By summing up the forces and taking the moment about the point where the left reaction force  $F_3$  is applied, both of the reaction forces  $F_3$  and  $F_4$  can be solved for in terms of the known forces  $F_1$  and  $F_2$  and the positions of all four forces using the following equations:

$$\sum F_z = F_3 + F_4 - F_1 - F_2 = 0 \quad \sum M_y = -F_1 d_{31} - F_2 d_{32} + F_4 d_{34} = 0 \quad (2)$$

where  $d_{ij}$  represents the distance from one force to another. Furthermore,  $F_1$  and  $F_2$  were both assumed to be half of the total force measured by the load cell. From this, the reaction forces were

calculated in terms of  $F_1$ ,  $F_2$ , and the distances between the loads.

$$F_3 = F_1 + F_2 - \frac{F_1 d_{31} + F_2 d_{32}}{d_{34}} \quad F_4 = \frac{F_1 d_{31} + F_2 d_{32}}{d_{34}} \quad (3)$$

The beam was then separated with five cuts, each corresponding to a section before or after each force was applied on the beam. The shear force and bending moments were then calculated for each cut.  $d_i (i = 1, 2, 3)$  represents the distance from the left of the beam to the respective force, while  $d_4$  represents the distance from the right reaction force to the right of the beam.

Cut 1:  $0 \leq x < d_3$

$$\sum V_z = 0 \quad \sum M_y = 0 \quad (4)$$

Cut 2:  $d_3 \leq x < d_1$

$$\sum V_z = F_3 \quad \sum M_y = F_3(x - d_3) \quad (5)$$

Cut 3:  $d_1 \leq x < d_2$

$$\sum V_z = F_3 - F_1 \quad \sum M_y = F_3(x - d_3) - F_1(x - d_1) \quad (6)$$

Cut 4:  $d_2 \leq x < d_4$

$$\sum V_z = -F_4 \quad \sum M_y = F_4(L - x - d_4) \quad (7)$$

Cut 5:  $d_4 \leq x < L$

$$\sum V_z = 0 \quad \sum M_y = 0 \quad (8)$$

The shear and bending moment diagrams are shown in Figure 8.

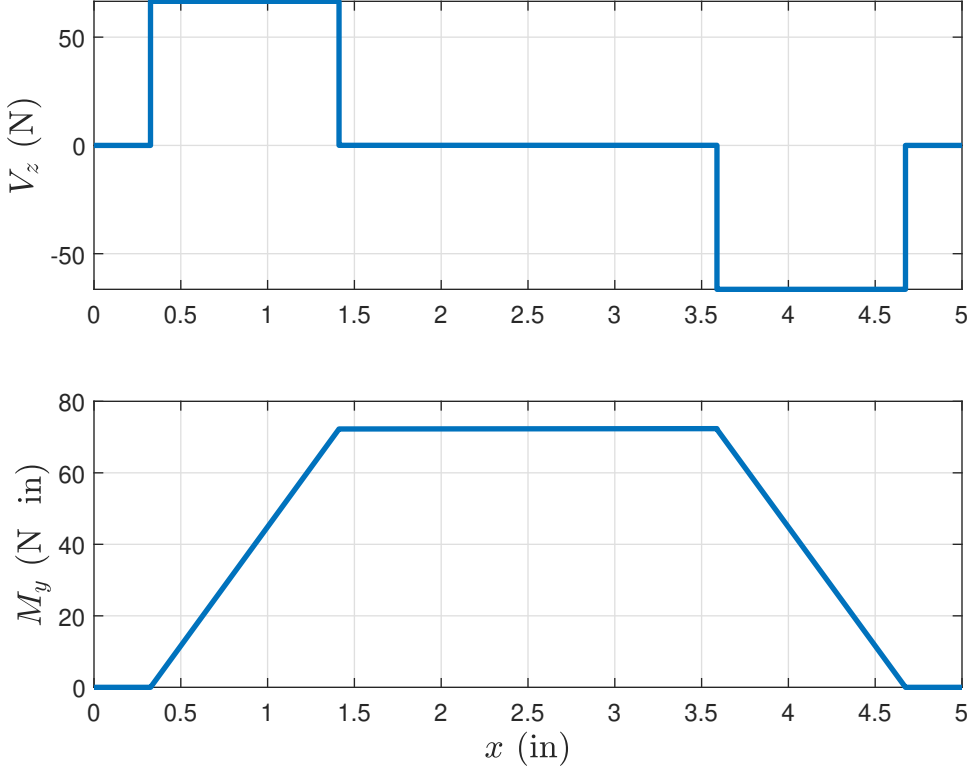


**Figure 8: Shear and Bending Moment Diagrams**

As can be seen from Figure 8, the shear force is approximately zero along that portion of the beam, as expected. In the case of pure bending, the maximum bending moment occurs when the shear force is zero, hence why the bending moment is maximum in that portion.

### 3.2 Fringe Constant

From the shear and bending moment diagrams, it is observed that the beam is in pure bending. Therefore, the stress can be related to the fringe constant using the relationship shown in Equation 9.

$$\sigma_1 - \sigma_2 = \sigma_x = \frac{f_\sigma}{t}(n) \quad (9)$$

where  $n$  represents the fringe order. Since this is a light-field, the dark fringes are half integers. The stress is related to the bending moment and moment of inertia by the following relationship:

$$\sigma_x = -\frac{M_y z}{I_{yy}} \quad (10)$$

where  $z$  represents the distance from the neutral axis. In this case,  $z$  represents the fringe location, or the distance from the top of the beam (where the maximum bending moment occurs) to the fringes. Using Equations 9 and 10, the stress vs. fringe order for the unnotched beam is obtained, as seen in Figure 9.

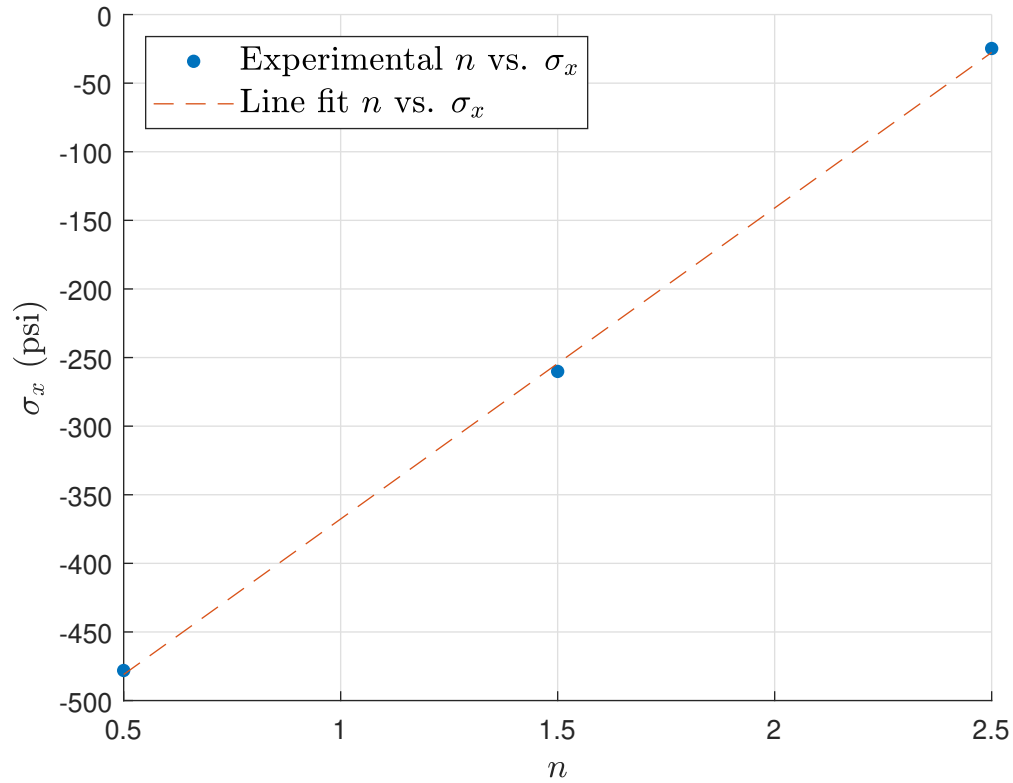


**Figure 9:**  $\sigma_x$  vs.  $n$  (fringe order) for the unnotched beam

A linear line of best fit was then applied to the data to obtain the slope, which represents  $\frac{f_\sigma}{t}$ . From this, the fringe constant was calculated to be 48.283 psi/in. Knowing the fringe constant allows the stress profiles for the notched beams to be calculated.

### 3.3 Stress Profile for U and V-Notch Beams

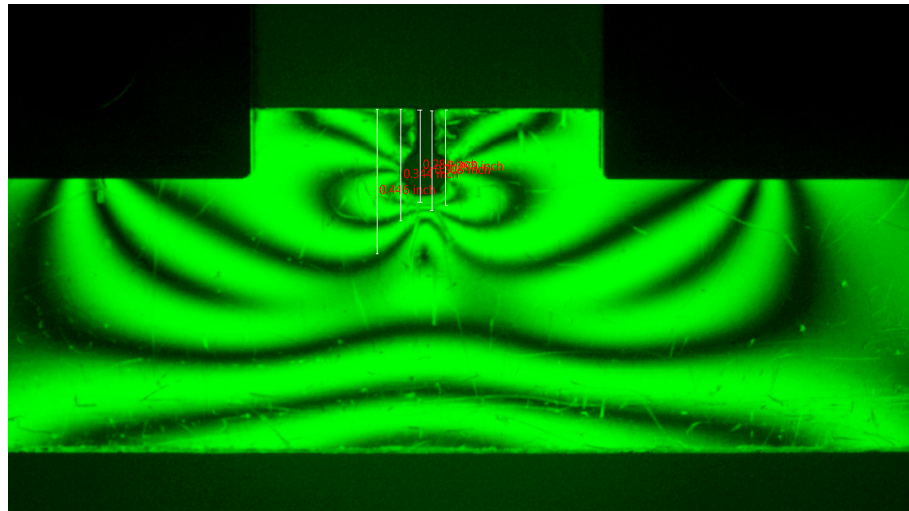


Figure 10: Light-field for the U-notch beam at a compressive force of 138 N

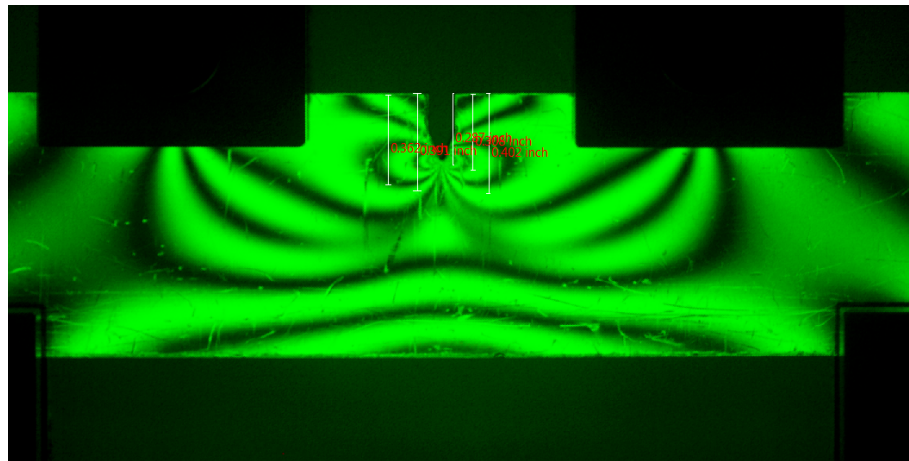
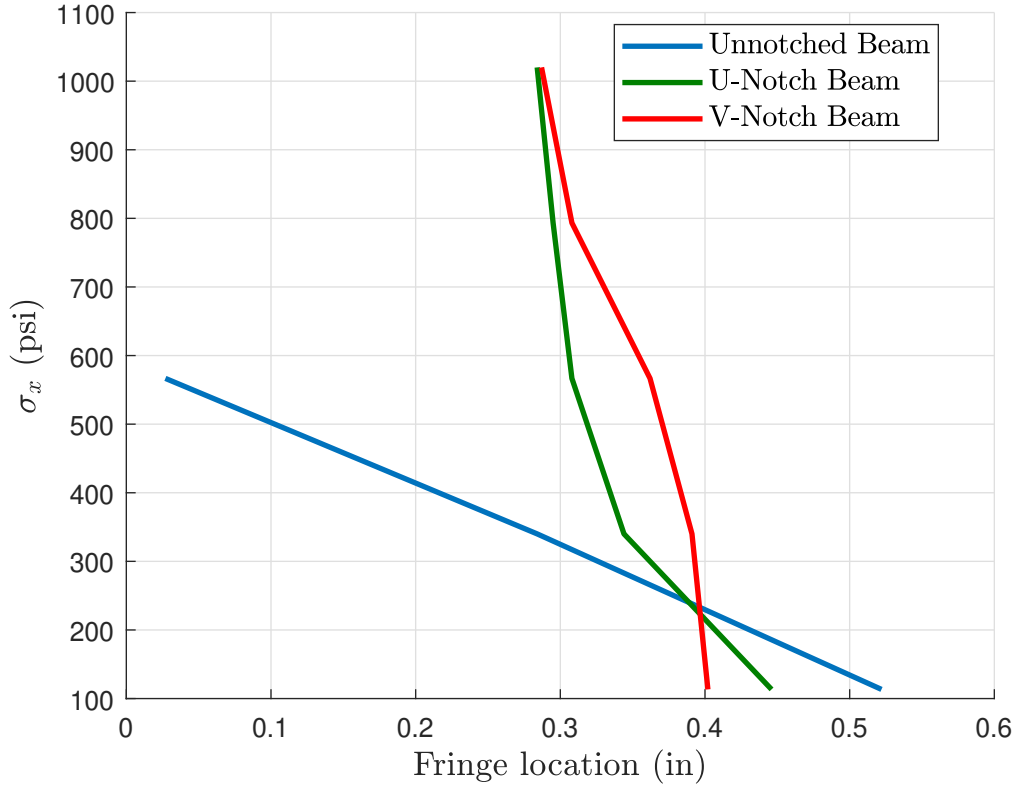


Figure 11: Light-field for the V-notch beam at a compressive force of 136 N

Figures 10 and 11 show a higher number of fringes closer to the edge of the notch. If the compressive force were to increase, more fringes would appear around the edge of the notch. This is due to the stress concentration factor, which will be addressed in a subsequent section. At lower fringe locations, the bending moment increases. Because stress is directly proportional to bending moment as seen in Equation 10, at lower fringe locations the stress will also increase. Also, Equation 9 shows that the stress is directly proportional to the fringe order; a higher fringe

order represents a larger stress. Because a higher dark-fringe order corresponds to a lower fringe location in a symmetric light-field, the stress profile is as expected.

Using the fringe constant, the stress profile for the notched beams can be obtained using Equation 9. The stress profile at different fringe locations is shown in Figure 12.



**Figure 12:**  $\sigma_x$  vs. fringe location for all three beams

As can be seen from Figure 12, the stress tends to zero as the fringe location gets higher for all three beams. This is to be expected, as the stress at the neutral axis is zero. Furthermore, the stress closer to the edges of the notches is extremely high. This is due to the stress concentration factor (addressed in the following section) causing the stress to be very high at holes. To emphasize this further, the stress profile for the U-Notched beam is plotted at measurements in the unnotched cross-section, shown in Figure 13. As the fringe location approaches the depth of the notch, the stress increases dramatically, and is linear up until that point.

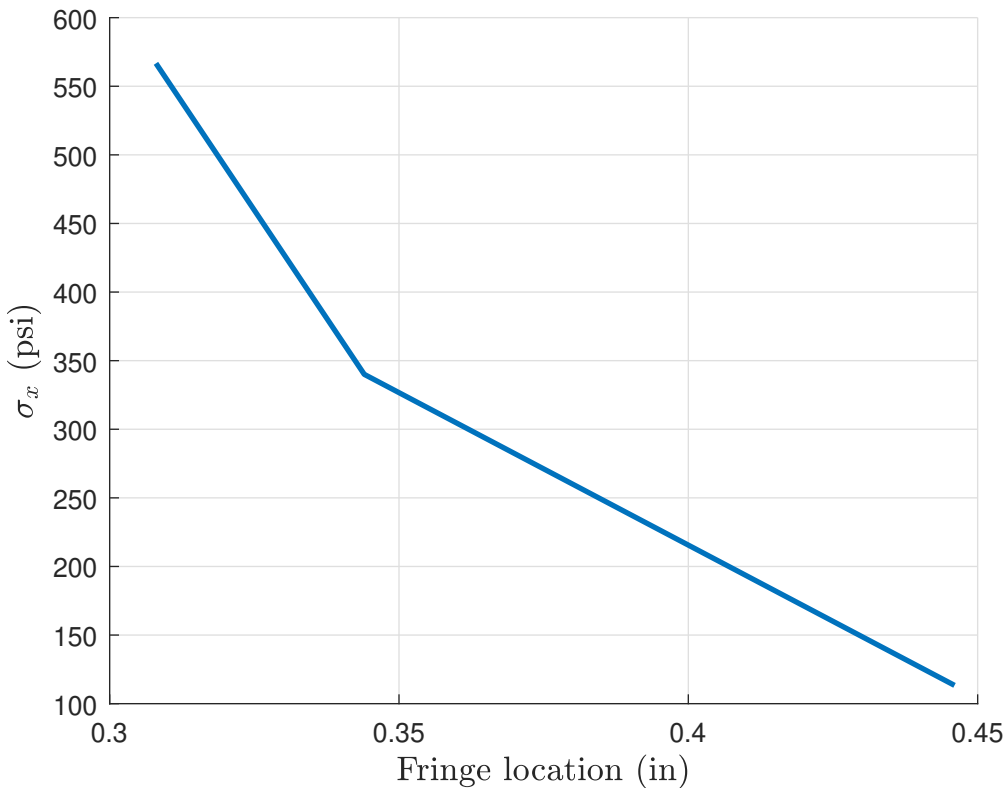


**Figure 13:**  $\sigma_x$  vs. fringe location for the U-Notch beam in the unnotched cross-section

### 3.4 Stress Concentration Factor

Photoelasticity is also useful when it comes to finding the maximum stress at a hole or notch. Theoretically, the maximum stress can be related to the nominal stress by the stress concentration factor,  $K_t$ . The relationship is shown in Equation 11.

$$\sigma_{max} = K_t \sigma_{nom}, \quad \sigma_{nom} = \frac{6M}{td^2} \quad (11)$$

However, often the stress concentration factor  $K_t$  is more complicated to calculate, as it depends on the depth, radius, and angle of a beam notch. Therefore, utilizing photoelasticity to obtain the maximum stress is preferable in this particular instance. Using a curve fit to extrapolate the stress at the edge of the notches, Figure 14 is obtained.

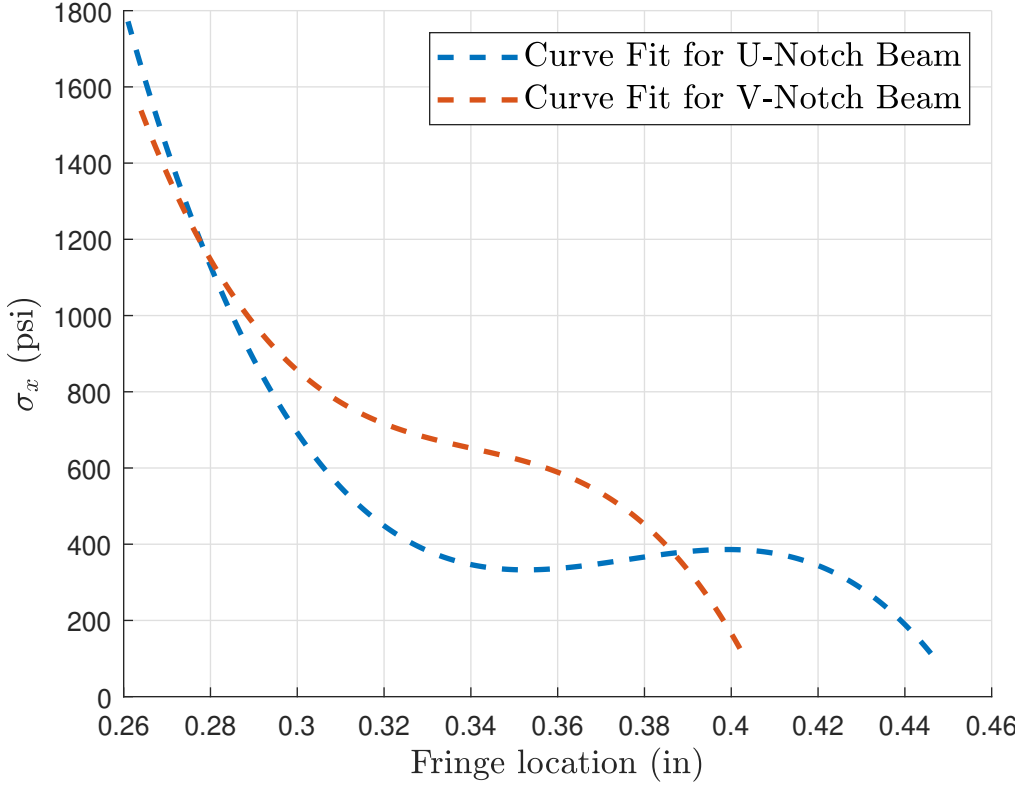


**Figure 14: Cubic curve fit for the U and V-Notch beams**

A cubic curve fit was used since the stress concentration factor is a cubic function. The theoretical maximum stress for the U and V-Notch beams were  $\sigma_{max} = 1732$  psi and  $\sigma_{max} = 1749$  psi respectively. The experimental maximum stress for the U and V-Notch beams were  $\sigma_{max} = 1772$  psi and  $\sigma_{max} = 1568$  psi respectively. The error is roughly 2% for the U-Notch beam and 10% for the V-Notch beam, which can be attributed to several factors. One major factor is the load cell; measurements taken with it tended to drift noticeably, exhibiting changes of up to  $\pm 20$  N. The beams could also have been mounted off center, which would affect the derived results from the beginning of the experiment. The applied compressive forces on the notched beams were also slightly different from the applied force on the unnotched beam; the moment used in the nominal stress calculation was obtained from the unnotched beam, so deviations in the applied forces on the notched beams as compared to the unnotched beam could lead to differing maximum stress values when compared to theoretical data. Furthermore, the curve fit was only applied to 5 data points, which may not be enough to determine an accurate extrapolation of a curve. However, obtaining

more data points requires a higher compressive force, which leads to plastic deformation beyond the yield stress. Finally, the notch and distance measurements may not be perfect; the image resolution and the need to manually measure points makes it difficult to obtain accurate measurements using Rincon HD.

#### 4. CONCLUSIONS

In this experiment, photoelasticity analysis was conducted on three different birefringent samples: one uniform beam, one with a small U-shaped notch, and one with a small V-shaped notch. By arranging quarter wave plates and the sample in a specific manner, the stress profile of each beam can be visualized and analyzed. The fringe constant was obtained from the unnotched beam's stress profile and used to get the stress profiles for the other two beams. For all three beams, the stress approaches zero as the fringe location increases. While all the beams had higher stresses at smaller fringe locations, the notched beams exhibited a significantly higher change in stress due to the stress concentration factor. The theoretical and experimental maximum stress were then calculated for both notched beams, which matched within reasonable error.

While this experiment was successful, a number of steps could be taken to perform the necessary processes more accurately. The most obvious change to make is to adjust the loading setup, including the load cell, to reduce the amount of drift in the measurements and increase the accuracy of load measurements. Another possible change is to collect more data points for the notched beams. With more data points, a more accurate fit for could be made for the notched beams, which would lead to a more accurate experimental maximum stress curve. However, if the compressive force is increased significantly, the material could experience yielding, driving it to plastic deformation beyond that point. One other improvement that could be made to the experiment is to use a camera with a higher resolution in order to improve the image quality, which would allow for more accurate measurements.

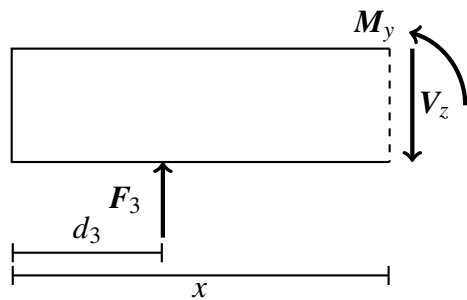
## 5. REFERENCES

- [1] Department of Materials Science. "Introduction to Photoelasticity." 2022. University of Cambridge, <https://www.doitpoms.ac.uk/tplib/photoelasticity/history.php>.
- [2] Department of Mechanical Engineering. "Photoelasticity". 2016. University of Washington, <https://depts.washington.edu/mictech/optics/me557/photoelasticity.pdf>.
- [3] "Measurement of Stress using Photoelasticity." Laboratory Write-up for AE 461, University of Illinois at Urbana Champaign, 2022.

## APPENDIX A. SAMPLE CALCULATIONS

### Shear Moment and Bending Moment for Cut 2

Taking the left cut along  $d_3 \leq x < d_1$ :



$$\sum F_z = 0 = V_z - F_3 \quad \rightarrow V_z = F_3$$

$$\sum M_y = 0 = M_y - F_3(x - d_3) \quad \rightarrow M_y = F_3(x - d_3)$$

### Stress at a fringe location for U-Notch beam

$$\sigma_x = \frac{f_\sigma}{t} n$$

$f_\sigma$  = fringe constant [Pa/m; psi/in]

$t$  = thickness of the beam [m; in]

$n$  = fringe order

Choosing  $n = 1.5$  which corresponds to a fringe location  $z = 0.344$  in and fringe constant  $f_\sigma = 48.2831$  psi/in and  $t = 0.215$  in:

$$\sigma_x = \frac{48.2831}{0.215}(1.5) = 336.86 \text{ psi}$$

### Stress Concentration Factor for U-Notch beam

$$K_t = C_1 + C_2 \left( \frac{h}{D} \right) + C_3 \left( \frac{h}{D} \right)^2 + C_4 \left( \frac{h}{D} \right)^3$$

where for  $2 \leq h/r \leq 20$ :

$$C_1 = 2.966 + 0.502h/r - 0.009(h/r)^2$$

$$C_2 = -6.475 - 1.126h/r + 0.019(h/r)^2$$

$$C_3 = 8.023 + 1.253h/r - 0.020(h/r)^2$$

$$C_4 = -3.573 - 0.634h/r + 0.010(h/r)^2$$

$h$  = depth of the notch [m; in]

$r$  = radius of the notch [m; in]

$D$  = width of the beam [m; in]

Using  $h = 0.146$  in,  $D = 1$  in,  $r = 0.1305$  in:

$$C_1 = 4.6458$$

$$C_2 = -10.2580$$

$$C_3 = 12.2472$$

$$C_4 = -5.7109$$

Then  $K_t = 2.0847$

## APPENDIX B. RAW DATA

### Unnotched Beam Stress Profile

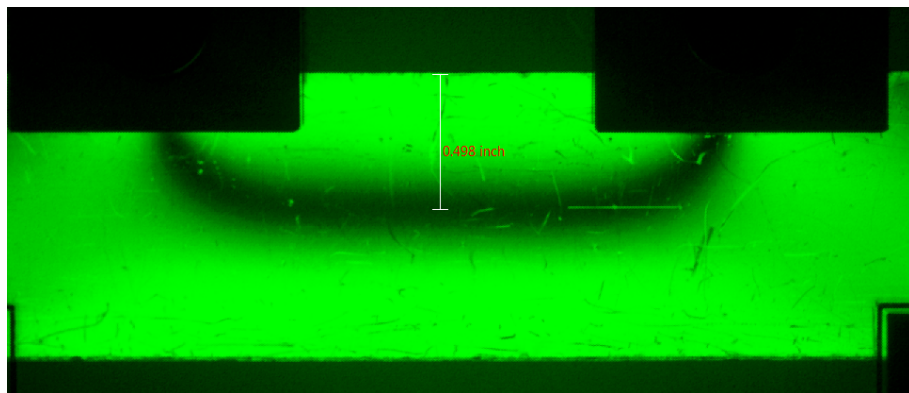


**Figure 15:** Unnotched beam light field at a compressive force of 35 N

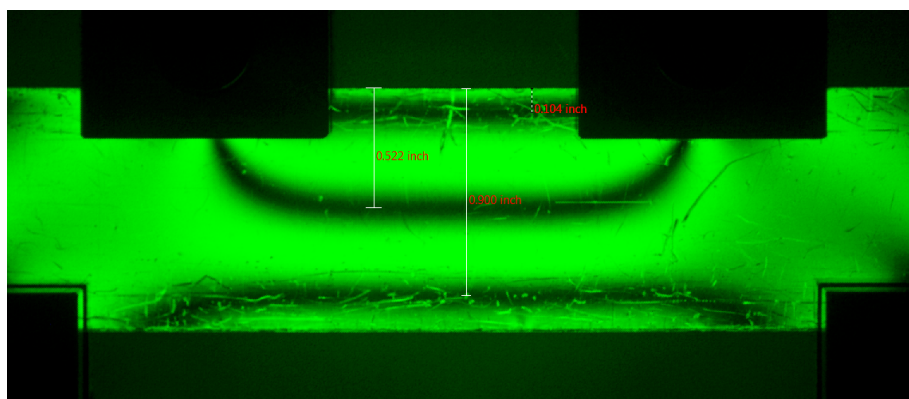


**Figure 16:** Unnotched beam light field at a compressive force of 78 N

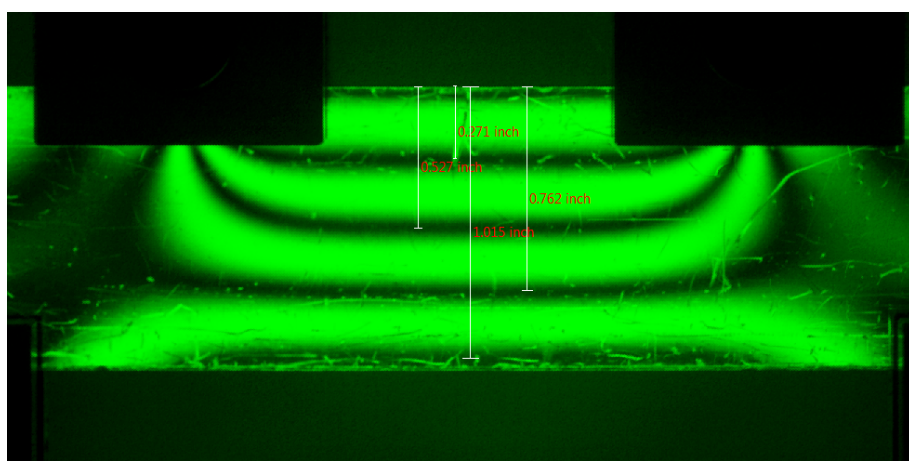


**Figure 17:** Unnotched beam light field at a compressive force of 126 N

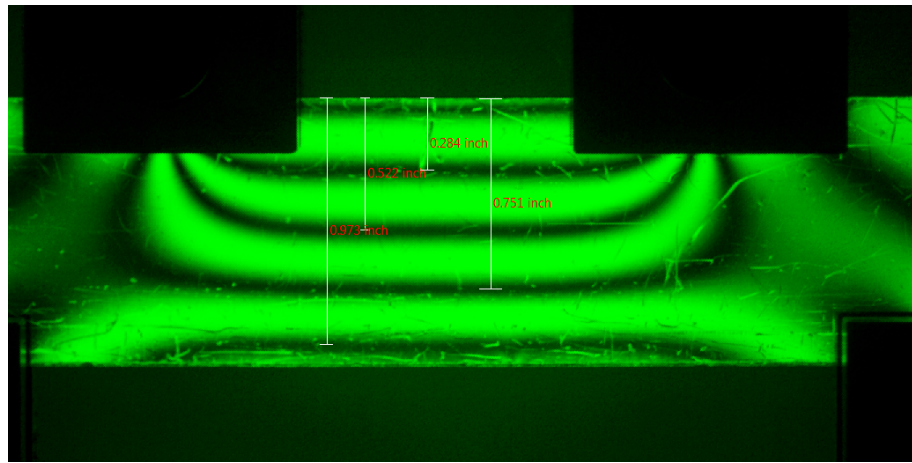


**Figure 18:** Unnotched beam light field at a compressive force of 133 N

#### U-Notch Beam Stress Profile

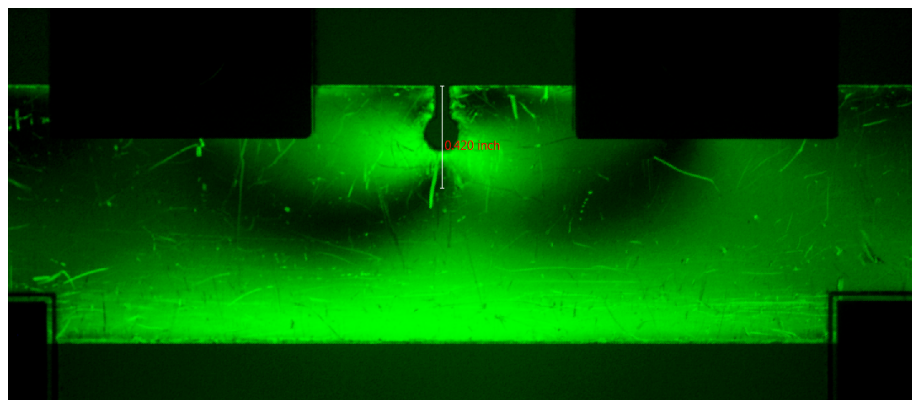


**Figure 19:** U-Notch beam light field at a compressive force of 14 N

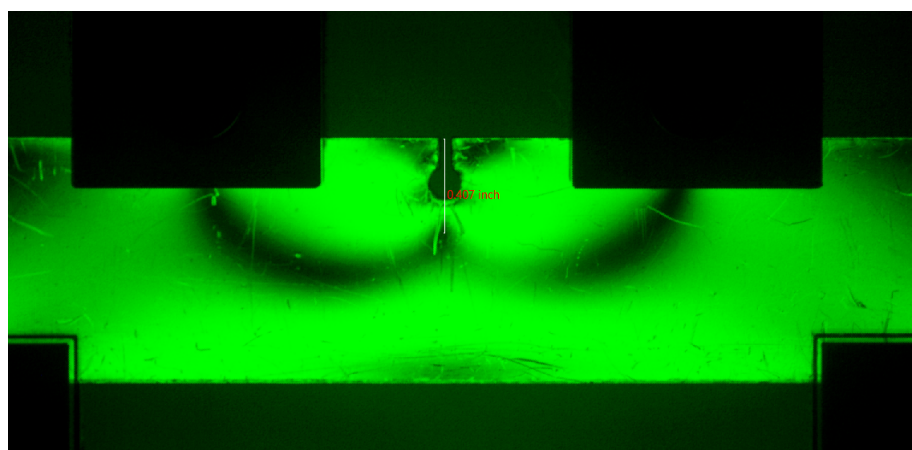


**Figure 20:** U-Notch beam light field at a compressive force of 36 N

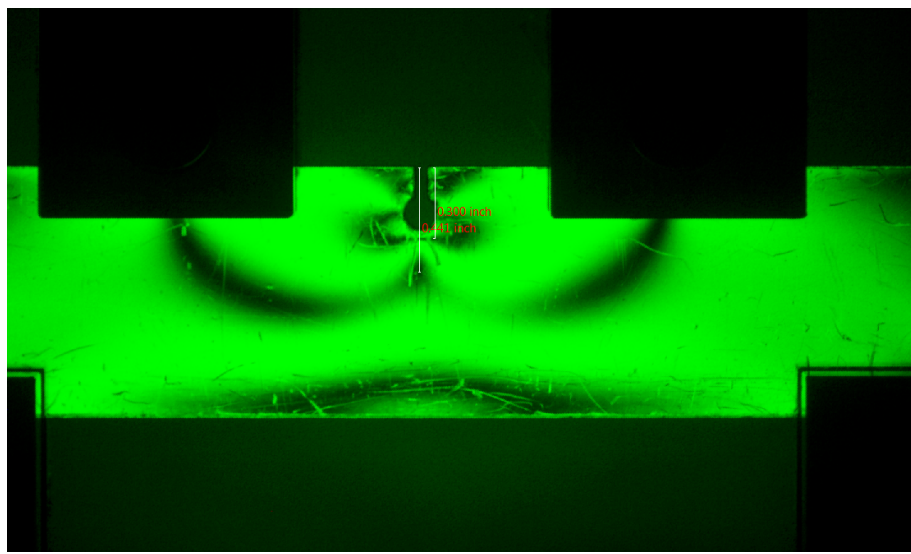


**Figure 21: U-Notch beam light field at a compressive force of 53 N**

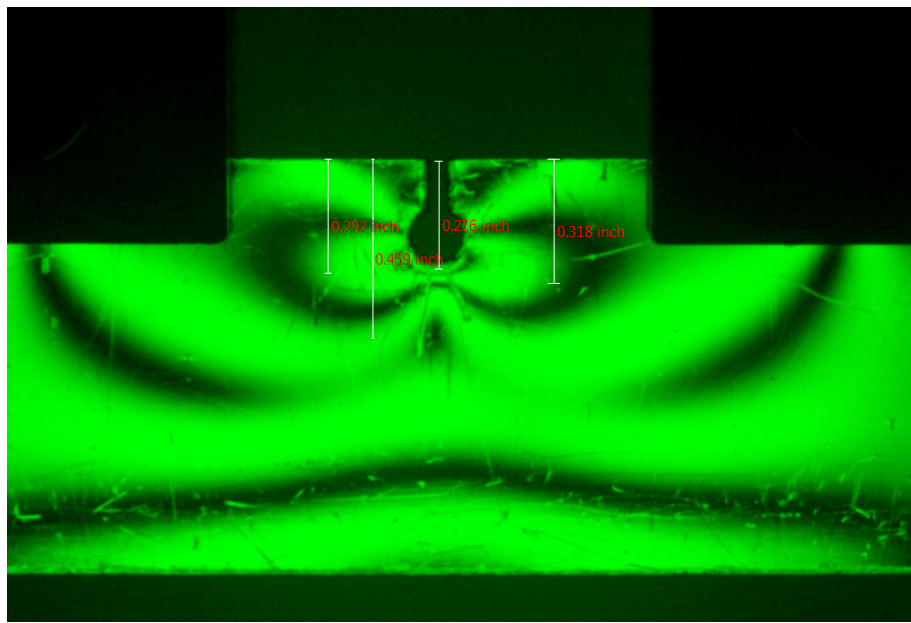


**Figure 22: U-Notch beam light field at a compressive force of 78 N**

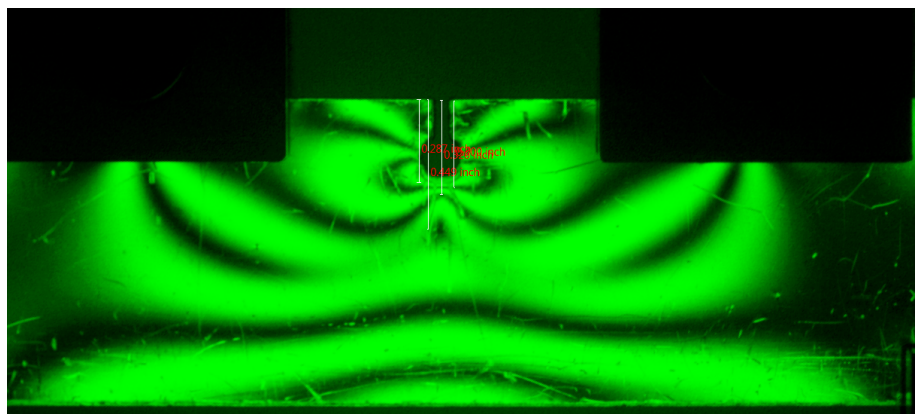


**Figure 23:** U-Notch beam light field at a compressive force of 105 N

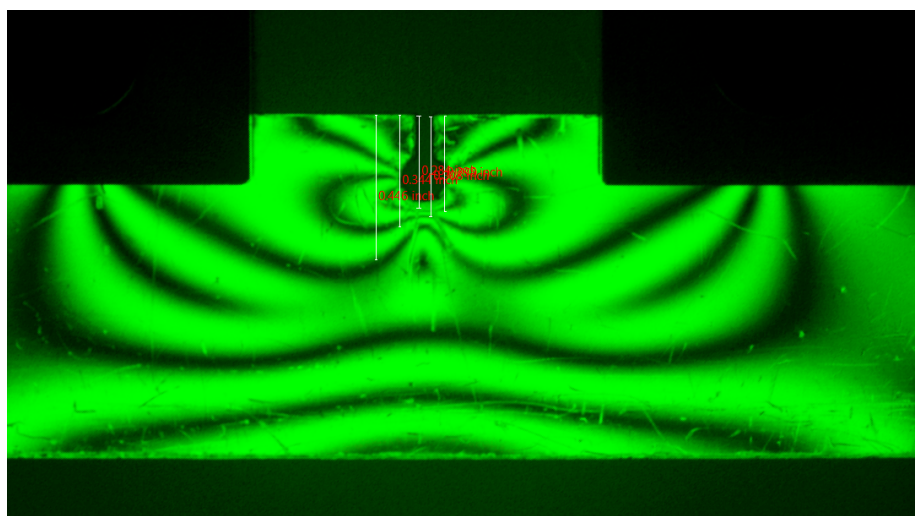


**Figure 24:** U-Notch beam light field at a compressive force of 138 N

### V-Notch Stress Profile

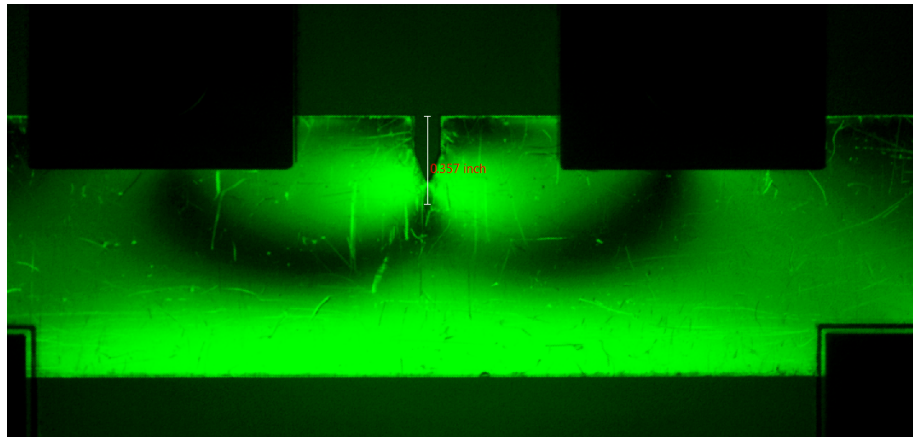


Figure 25: V-Notch beam light field at a compressive force of 16 N

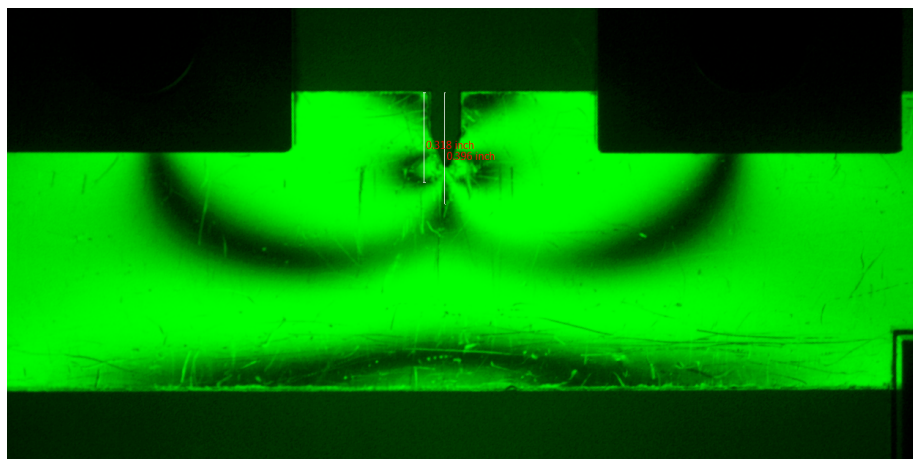


Figure 26: V-Notch beam light field at a compressive force of 49 N

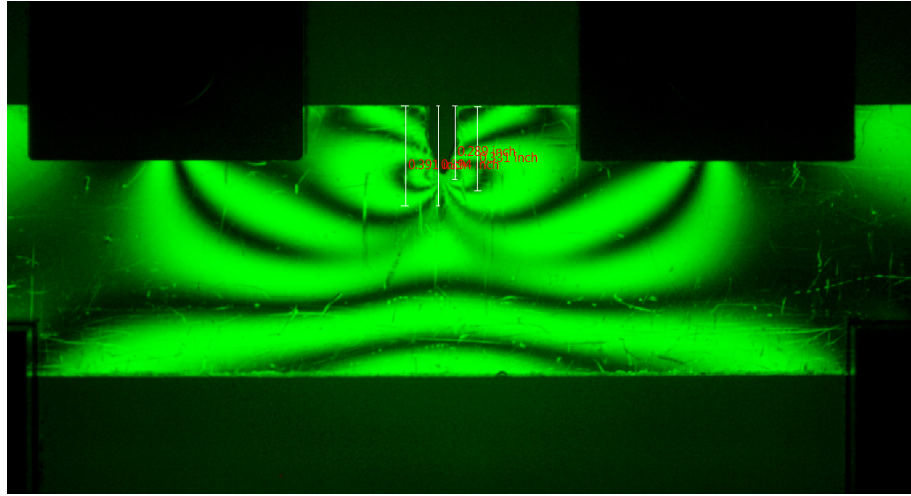


Figure 27: V-Notch beam light field at a compressive force of 100 N

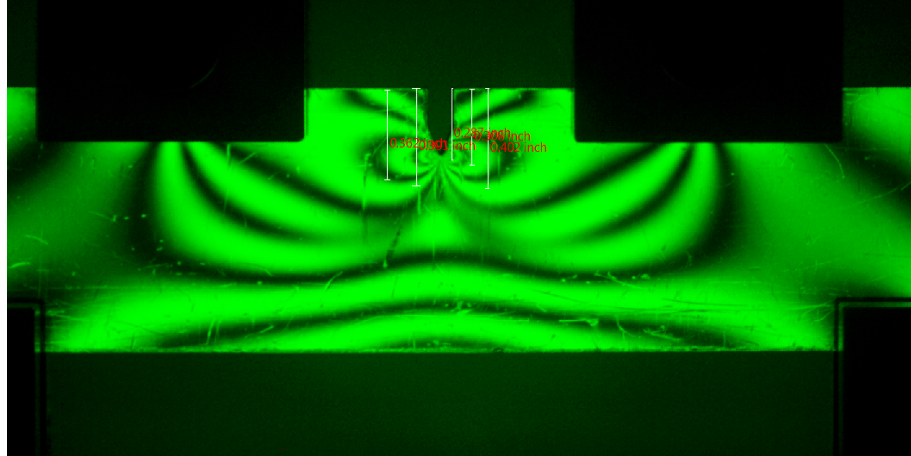


Figure 28: V-Notch beam light field at a compressive force of 136 N

## APPENDIX C. CODE

---

```
1 clear all; clc; close all
2
3 %% Shear Force and Bending Moment Diagrams
4 d12 = 2.177 % in;
5 d34 = 4.349 % in;
6 dR1F1 = 1.0846 % in;
7 dR2F2 = 1.095 % in;
8 L = 5 % in;
9
10 dF1 = 0.5*(L - d12);
11 dR1 = 0.5*(L - d34);
```

```

12
13 dF2 = dF1 + d12;
14 dR2 = dR1 + d34;
15
16 syms R1 R2
17 F = 133 % N;
18 F1 = F/2;
19 F2 = F/2;
20
21 eq1 = 0 == R1 + R2 - F1 - F2;
22 eq2 = 0 == -F1*dR1F1 - F2*(d12 + dR1F1) + R2*d34;
23
24 soln = solve([eq1, eq2], [R1 R2]);
25 R1 = double(soln.R1);
26 R2 = double(soln.R2);
27
28 % Number of points
29 N = 1001;
30 x1 = linspace(0, dR1, N);
31 x2 = linspace(dR1, dF1, N);
32 x3 = linspace(dF1, dF2, N);
33 x4 = linspace(dF2, dR2, N);
34 x5 = linspace(dR2, L, N);
35
36 figure(1), clf;
37
38 subplot(2, 1, 1);
39 plot([x1, x2, x3, x4, x5], [zeros(1, N), R1*ones(1, N), (R1 - F1)*ones(1, N), ...
40 -R2*ones(1, N), zeros(1, N)], 'linewidth', 2)
41 grid on;
42 ylabel('$V_z$ (N)', 'Interpreter', 'latex', 'FontSize', 13)
43
44 subplot(2, 1, 2);
45 plot([x1, x2, x3, x4, x5], [zeros(1, N), R1*(x2 - dR1), R1*(x3 - dR1) - F1*(x3 - dF1), ...
46 R2*(L - x4 - dR1), zeros(1, N)], 'linewidth', 2)
47 grid on;
48 ylabel('$M_y$ (N \ in)', 'FontSize', 13, 'Interpreter', 'latex')
49 xlabel('$x$ (in)', 'interpreter', 'latex', 'fontsize', 13)
50 saveas.figure(1, 'ShearBending.eps', 'epsc')
51
52 %% Calculating the fringe constant
53 t = 0.213 % in;
54 h = 1 % in;
55 Iyy = 1/12 * t * h^3 % in^4;
56

```

```

57 z = [0.522, 0.284, h - 0.973]; % Fringe locations for the unnotched beams (in)
58 m = [0.5, 1.5, 2.5] % Fringe order;
59 M = 72.3145*0.2248089431; % lbs-in
60
61 sigmaX = zeros(1, length(z));
62
63 for i=1:length(z)
64     sigmaX(i) = -M*z(i)/Iyy;
65 end
66
67 p = polyfit(m, sigmaX, 1);
68 % Fringe constant
69 Fs = p(1)*t;
70
71 % Line fit fringe order vs stress
72 mFit = linspace(m(1), m(end), N);
73 sigmaXFit = polyval(p, mFit);
74
75 figure(2), clf, hold on, grid on;
76 plot(m, sigmaX, '.', 'MarkerSize',15)
77 plot(mFit, sigmaXFit, '--')
78 xlabel('$n$', 'FontSize',13, 'Interpreter','latex')
79 ylabel('$\sigma_x$ (psi)', 'FontSize', 13, 'Interpreter','latex')
80 legend({'Experimental $n$ vs. $\sigma_x$', 'Line fit $n$ vs. $\sigma_x$'}, ...
81 'Interpreter','latex', 'FontSize', 13, 'Location','northwest')
82 saveas(figure(2), 'Fs.eps', 'epsc')
83 %% U-Notch, V-Notch Stress Resolution at F = 138, 136 N respectively
84 zU = [0.446, 0.344, 0.308, 0.295, 0.284];
85 mU = 0.5:1:length(zU) + 0.5;
86 sigmaU = zeros(1, length(zU));
87
88 zV = [0.402, 0.391, 0.362, 0.308, 0.287];
89 mV = mU;
90 sigmaV = zeros(1, length(zV));
91
92 sigmaUn = zeros(1, length(z));
93
94 for i=1:length(zU)
95     sigmaU(i) = Fs/t * mU(i);
96     sigmaV(i) = Fs/t * mV(i);
97 end
98
99 for i=1:length(z)
100    sigmaUn(i) = Fs/t * m(i);
101 end

```

```

102
103 figure(3), clf, hold on, grid on;
104 set(gca,'DefaultLineLineWidth',2)
105 plot(z, sigmaUn)
106 plot(zU, sigmaU, 'color', [0 0.5 0])
107 plot(zV, sigmaV, 'r')
108 xlabel('Fringe location (in)', 'Interpreter','latex', 'FontSize',13)
109 ylabel('$\sigma_x$ (psi)', 'Interpreter','latex', 'FontSize',13)
110 legend({'Unnotched Beam', 'U-Notch Beam', 'V-Notch Beam'}, 'Interpreter','latex', ...
111 'fontsize', 11, 'Location','best')
112 saveas(figure(3), 'StressVFringleLocation.eps', 'epsc')

113
114 figure(4), clf, hold on, grid on;
115 plot(zU(1:end-2), sigmaU(1:end-2), 'LineWidth',2)
116 xlabel('Fringe location (in)', 'Interpreter','latex', 'FontSize',13)
117 ylabel('$\sigma_x$ (psi)', 'Interpreter','latex', 'FontSize',13)
118 saveas(figure(4), 'StressVsUnnotchedCross.eps', 'epsc')
119 %% Theoretical Maximum Stress for U and V Notched Beams
120 tU = 0.215; % thickness of the U notch beam (in);
121 tV = 0.214; % thickness of the V notch beam (in);
122
123 depthU = 0.261; % depth of the U notch (in)
124 depthV = 0.263; % depth of the V notch (in)
125
126 dU = h - depthU;
127 dV = h - depthV;
128
129 rU = 0.146/2; % radius of the U notch (in)
130
131 sigma_Nom_U = 6*M/(tU*dU^2);
132 sigma_Nom_V = 6*M/(tV*dV^2);
133
134 % U-Notch
135 % Since h/r is greater than 2 and less than 20
136 C1 = 2.966 + 0.502*depthU/rU - 0.009*(depthU/rU)^2;
137 C2 = -6.475 - 1.126*depthU/rU + 0.019*(depthU/rU)^2;
138 C3 = 8.023 + 1.253*depthU/rU - 0.020*(depthU/rU)^2;
139 C4 = -3.572 - 0.634*depthU/rU + 0.010*(depthU/rU)^2;
140
141 % Stress concentration factor
142 KtU = C1 + C2*(depthU/h) + C3*(depthU/h)^3 + C4*(depthU/h)^5;
143 sigma_Max_U = KtU*sigma_Nom_U;
144
145 % V-Notch
146 KtV = KtU;

```

```

147 sigma_Max_V = KtV*sigma_Nom_V;
148
149 % Curve fitting to extrapolate maximum stress
150 zUFit = linspace(zU(1), depthU, N);
151 zVFit = linspace(zV(1), depthV, N);
152 % Cubic fit since the stress concentration factor is cubic
153 pUFit = polyfit(zU, sigmaU, 3);
154 pVFit = polyfit(zV, sigmaV, 3);
155
156 sigmaUFit = polyval(pUFit, zUFit);
157 sigmaVFit = polyval(pVFit, zVFit);
158
159 errorU = abs(sigma_Max_U - max(sigmaUFit))/sigma_Max_U
160 errorV = abs(sigma_Max_V - max(sigmaVFit))/sigma_Max_V
161
162 figure(5), clf, hold on, grid on;
163 set(gca,'DefaultLineLineWidth',2)
164 plot(zUFit, sigmaUFit, '--')
165 plot(zVFit, sigmaVFit, '--')
166 xlabel('Fringe location (in)', 'FontSize',13, 'Interpreter','latex')
167 ylabel('$\sigma_x$ (psi)', 'FontSize', 13, 'Interpreter','latex')
168 legend({'Curve Fit for U-Notch Beam', 'Curve Fit for V-Notch Beam'}, ...
169 'Interpreter','latex', 'FontSize',13)
170 saveas(figure(5), 'CurveFitStress.eps', 'epsc')

```

---

## APPENDIX D. GROUP MEMBER CONTRIBUTIONS

Name	Written Sections	Tables	Figures	Comments
Felix Marrar	3, Appendix A, Appendix C		8, 9, 12, 13, 14	Wrote all the code for calculations, analysis, and sample calculations
Quang Do	3, 4			Main collaborator on Section 3 and analysis, revised report wording/structure
Jason Chen	1, 2	1	3,4,5,6	Made the apparatus images, and table
Shanit Dev	1, 3			Rewrote some sentences in Section 3 and 1
Michael Biela	4			
Jamal Zain	1,4			